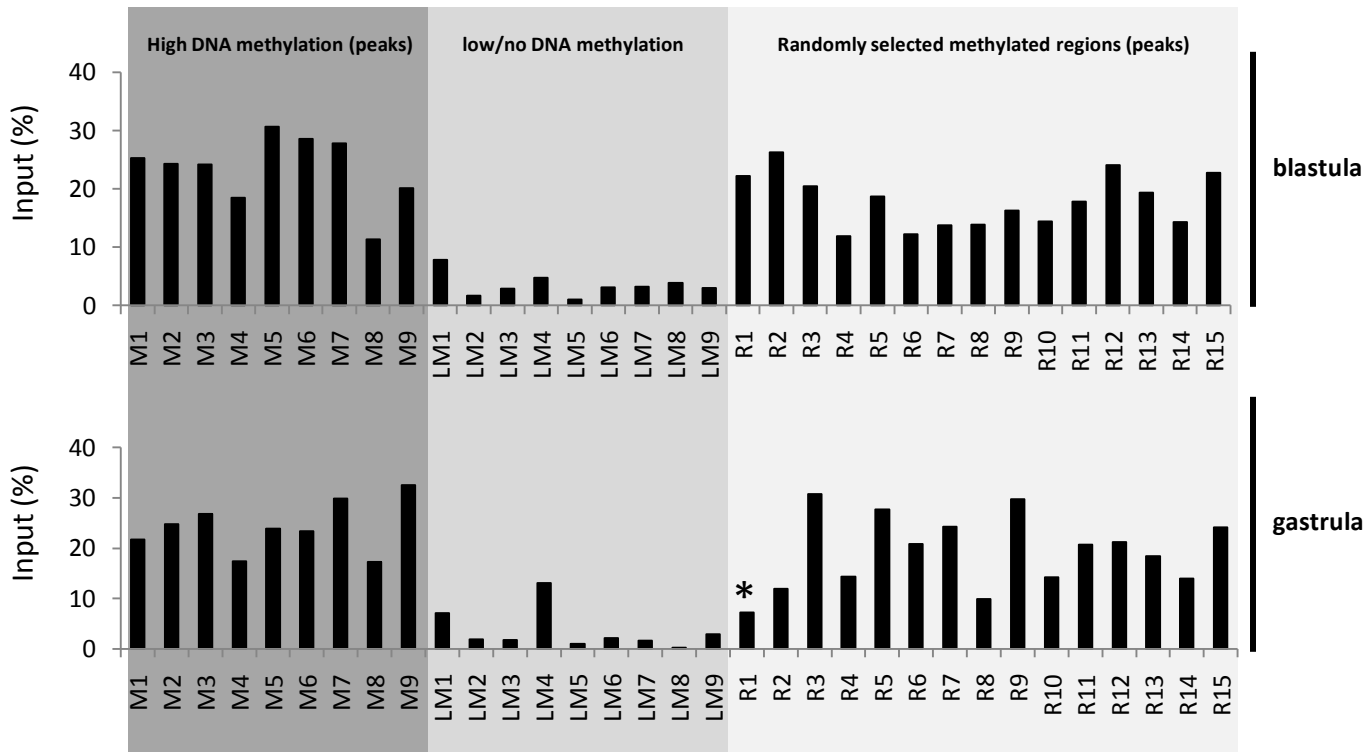


A



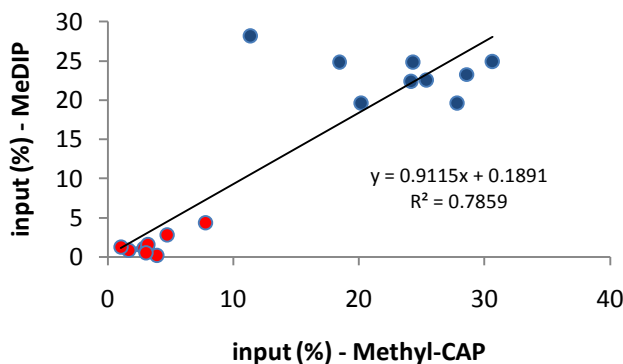
B

R1	scaffold_88:1,787,610-1,787,746
R2	scaffold_133:1,374,577-1,374,665
R3	scaffold_1226:67,469-67,604
R4	scaffold_106:1,200,309-1,200,451
R5	scaffold_435:603,740-603,846
R6	scaffold_399:4,184-4,313
R7	scaffold_527:184,868-185,008
R8	scaffold_724:407,383-407,528
R9	scaffold_556:584,592-584,713
R10	scaffold_892:161,488-161,631
R11	scaffold_372:420,320-420,466
R12	scaffold_205:896,507-896,651
R13	scaffold_105:769,370-769,490
R14	scaffold_705:83,104-83,247
R15	scaffold_181:1,766,488-1,766,636
M1	scaffold_780:402,274-402,403
M2	scaffold_3302:2,169-2,294
M3	scaffold_166:2,046,701-2,046,826
M4	scaffold_94:2,216,508-2,216,601
M5	scaffold_1162:96,447-96,549
M6	scaffold_12:733,442-733,583
M7	scaffold_760:256,665-256,772
M8	scaffold_967:214,278-214,387
M9	scaffold_845:321,690-321,839
LM1	scaffold_22:1,269,883-1,270,009
LM2	scaffold_339:854,219-854,308
LM3	scaffold_174:1,948,123-1,948,263
LM4	scaffold_42:2,252,812-2,252,960
LM5	scaffold_131:1,964,705-1,964,819
LM6	scaffold_38:3,799,594-3,799,737
LM7	scaffold_37:1,005,241-1,005,370
LM8	scaffold_917:263,956-264,088
LM9	scaffold_76:1,138,609-1,138,757

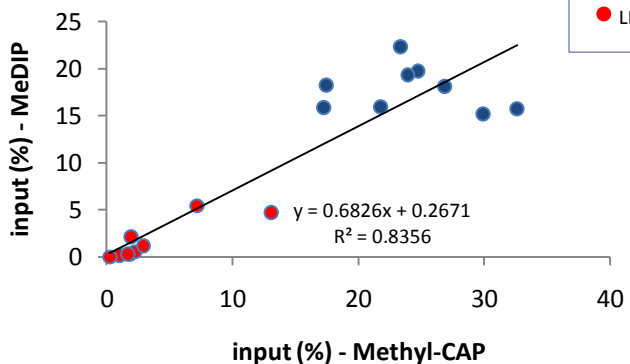
Figure S1. Quantitative PCR validation of methylated regions (peaks) obtained by massive parallel sequencing. **(A)** Highly methylated peaks (M1-M9), regions with low/no methylation (L1-L9) and randomly selected peaks of DNA methylation (R1-R15) were subjected to quantitative PCR after affinity precipitation (MethylCap, 500mM elution). The regions with low/no DNA methylation were used to determine the background level of the DNA methylation capture technique. 15 out of 15 randomly selected targets were verified as true positives (> 2.5 times over background, FDR < 0.067) in the blastula stage, while in the gastrula stage 14 out of 15 targets tested positive (FDR = 0.067) **(B)** Genomic locations of amplicons used for peak validation.

A

blastula (st.9)

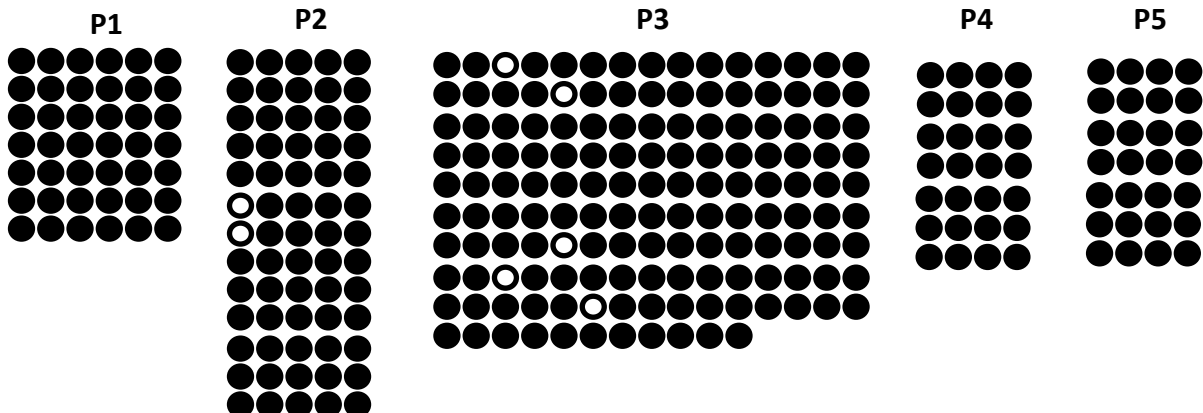


gastrula (st.12.5)



● M1-M9
● LM1-LM9

B

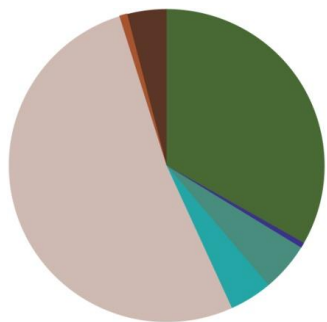


C

P1F: TAATGTAGGAGAATTAATTATTG	scaffold_369:202,717-202,841
P1R: AATATCATCTTATAAATCTAATAACAA	
P2F: GGTATATTTAGTGTGGGTTTATT	scaffold_1028:36,895-37,037
P2R: CTACCACATATTAACAAAAATAATT	
P3F: TTTATTATTGTTAATGAAGTTTTG	scaffold_1250:76,238-76,407
P3R: AAATCCCTCTAAACATCAACTC	
P4F: TTTTGTGTGGTTTTGGTAGTAG	scaffold_28:103,475-103,622
P4R: AACCCACAAAAACCTTCACTAATC	
P5F: AATGTGATGTTTGATATAGAAATT	scaffold_235:934,305-934,431
P5R: AAACTACAACAAATAATCTCCCC	

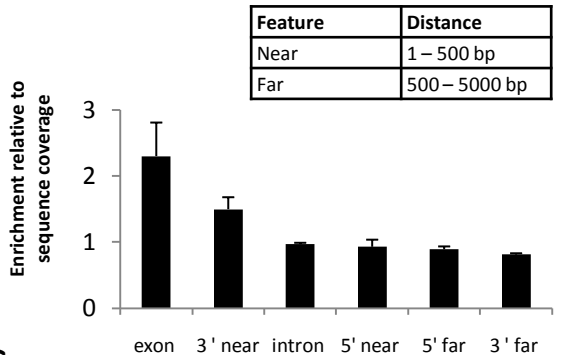
Figure S2. (A) Comparison of two different DNA methylation enrichment techniques. Results obtained by quantitative PCR after enrichment for DNA methylation by either MethylCap (affinity precipitation) or MeDIP (immunoprecipitation) show a significant degree of correlation (R^2 st9= 0.7859, R^2 st12.5= 0.8356). The primers used correspond to either highly methylated peaks (M1-M9) or regions with low/no methylation (LM 1-9). Genomic DNA from either blastula or gastrula stage was used as input. **(B)** Validation of randomly selected MethylCap peaks by bisulfite sequencing. Black circles represent methylated CpGs whereas white circles represent unmethylated ones. Rows of circles represent different sequenced clones. P1-P5 stands for PCR amplicons located within MethylCap peaks. All the examined peaks were robustly methylated at late gastrula. **(C)** Genomic locations and primer sequences of peaks examined by bisulfite sequencing.

A



- intron
- 5' near (1-500 bp)
- 5' far (500-5000 bp)
- 3' far (500-5000 bp)
- distant (5000- bp)
- 3' near (1-500bp)
- exon

B



C

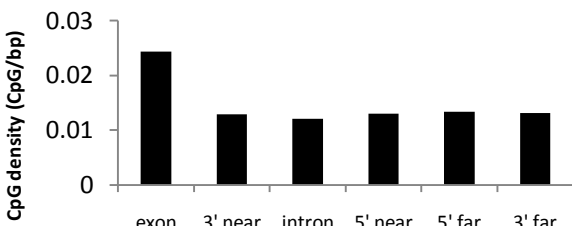
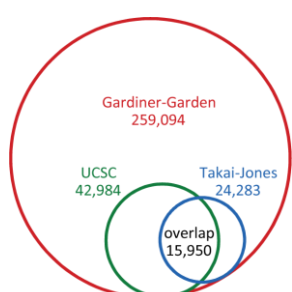
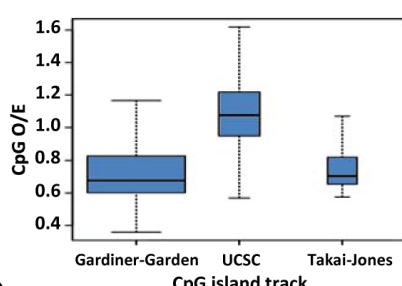


Figure S3. (A) Genomic distribution of DNA methylation peaks relative to genes as determined by the PinkThing software. The pie chart represents the genomic distribution average of the four peak files. (B) Genomic distribution of DNA methylation normalized for feature length. Error bars represent the standard deviation of the four DNA methylation data sets. (C) CpG density (CpG/bp) of distinct genomic features.

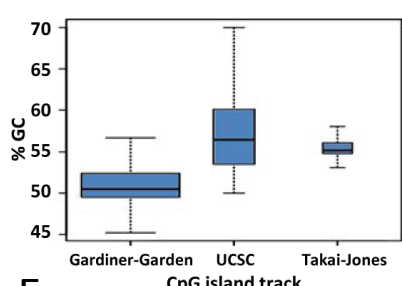
A



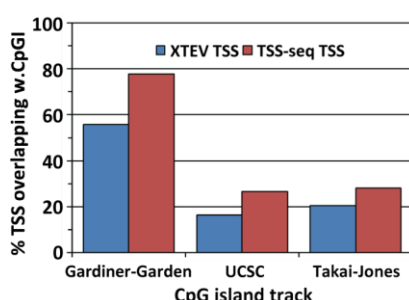
B



C



D



E

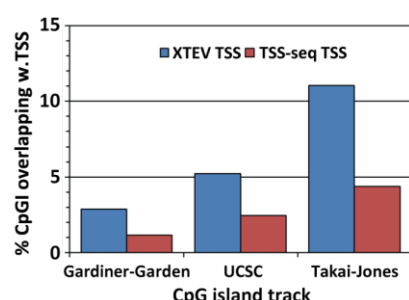


Figure S4. Comparison of CpG island (CpGi) collections obtained using different CpGi criteria (Takai-Jones, Gardiner-Garden, see main text). UCSC refers to the CpGi track downloaded from the UCSC genome browser. (A) Venn diagram showing overlaps between three different CpGi tracks. (B) Differences in the ratio of observed/expected CpG dinucleotides between different tracks (C) Differences in GC content between distinct CpGi tracks. (D and E) Genomic intersection of CpGis and transcription start sites (TSSs) belonging to XTEV gene models or TSSs validated by TSS-seq (Van Heeringen, 2011). (D) Percentage of TSSs overlapping with CpGis. (E) Percentage of CpGis overlapping with TSSs. The Takai-Jones CpGi track is the most enriched for TSSs.

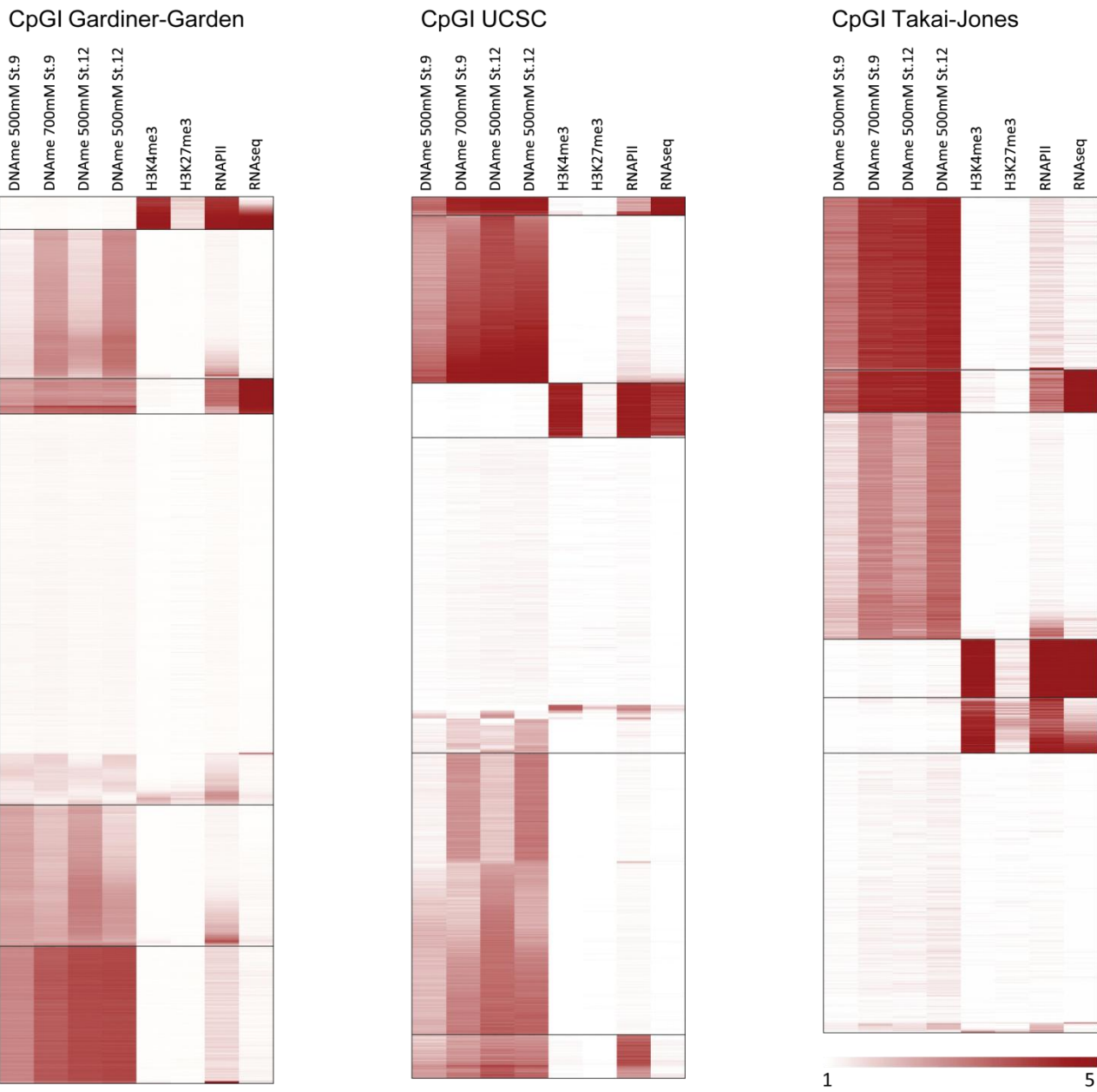


Figure S5. K-means clustering ($k=6$) performed on CpG islands obtained by different CpGI calling protocols: (1) Gardiner-Garden, (2) Takai-Jones and (3) CpG island track at the UCSC genome browser (see main text). Total number of DNA methylation, histone methylation, RNAPII and RNA tags was mapped to CpG islands and k-means clustering was performed. Independently of the CpGI collection used, similar clusters were obtained. For example, all three CpGI collection display a population of: a) active promoters (H3K4me3, RNAPII, RNAseq, no DNA methylation), b) exons of expressed genes (DNA methylation, RNAseq, RNAPII), c) introns of expressed genes (DNA methylation, RNAPII, no RNAseq) and d) unmethylated CpGis without RNAPII or histone modifications.

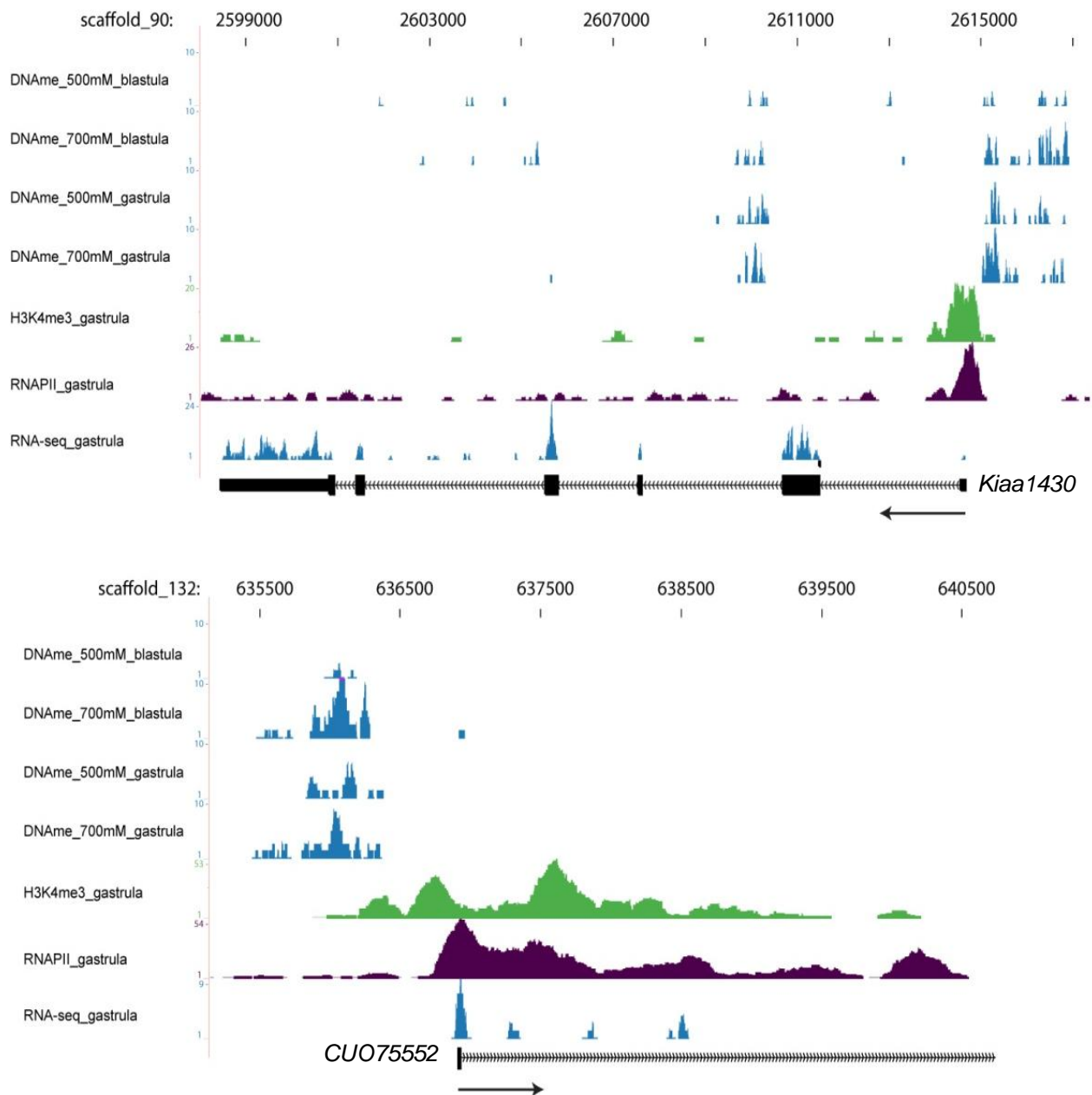
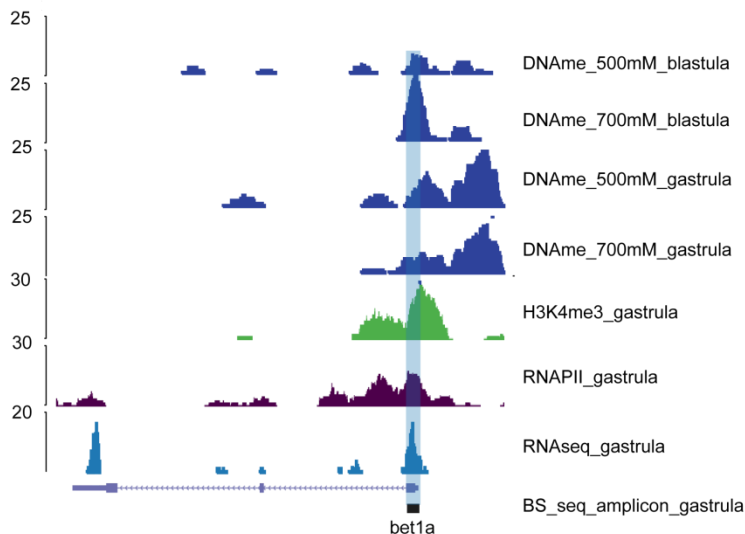
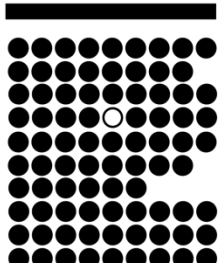


Figure S6. Two examples of active genes (*Kiaa1430* and *CUO75552* *x. tropicalis* mRNA) displaying robustly methylated upstream promoter regions through blastula and gastrula stages. In total, 865 expressed genes were found to contain DNA methylation in upstream promoter regions (TSS – 1kb) (see supplemental table S8).

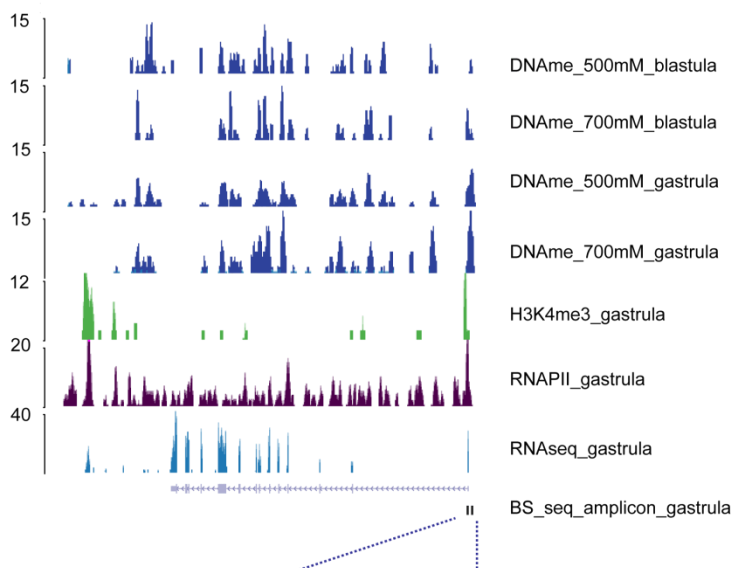
A

BET1 scaffold_104

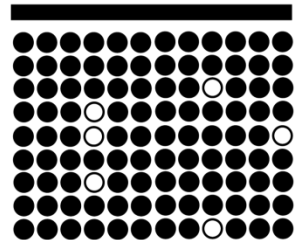
bet1a



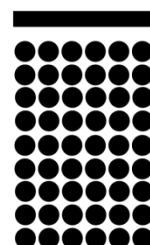
B

c20orf151 scaffold_531

c20-1



c20-2



C

Bet1A-F	TGGTTTTATTTAGGTTTAGTTATT
Bet1A-R	ATAACTACCTACTCTTCCTTCCTTAA
C20-1_F	TATAGTGTAGTGTGAATATAAAAGTAGG
C20-1_R	AAAATTATTAACAATTATCTCCATTAC
C20-2_F	GGGTTTGTTGTTAATAAAAGTG
C20-2_R	ACACAAATCTATAAAATTCTCCCC

Figure S7. Bisulfite sequencing of *Bet1* and *C20orf151* loci. Black circles represent methylated CpGs whereas white circles represent unmethylated ones. **(A)** The *Bet1* locus is heavily methylated at its TSS even though the *Bet1* gene is expressed during gastrulation. **(B)** Both the *C20orf151* TSS (primer C20-1) and a region located immediately upstream of the TSS (C20-2) are robustly methylated. The RNAseq profile indicates that *C20orf151* is highly expressed during gastrulation. **(C)** Primer sequences used for bisulfite sequencing

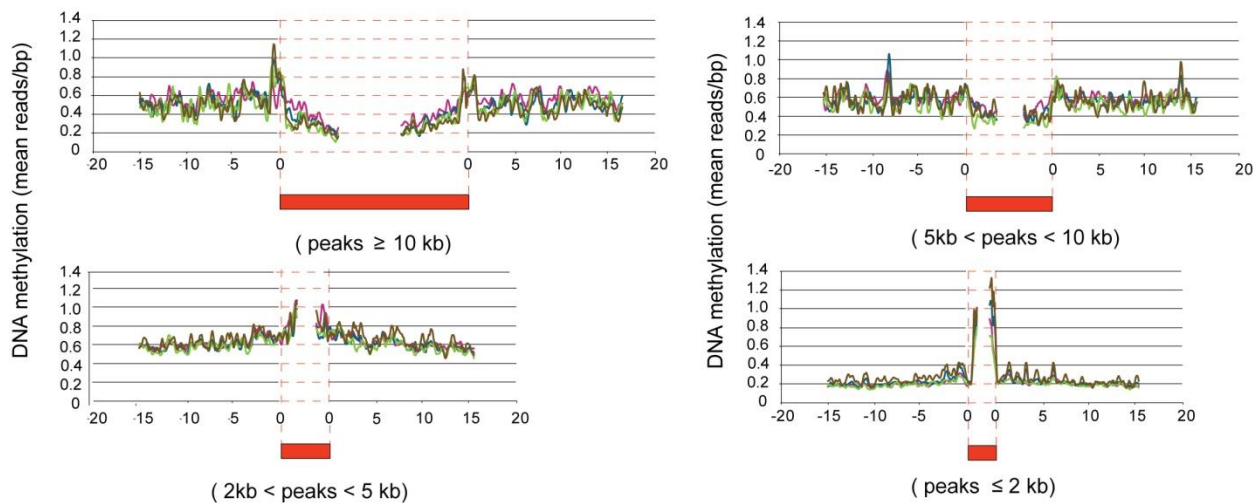


Figure S8. Profiles of DNA methylation over H3K27me3 peaks. Peaks were grouped into four bins depending on the H3K27me3 peak size. While large H3K27me3 peaks (> 5 kb) show a clear depletion in the average number of DNA methylation reads, smaller peaks (< 5 kb) are enriched for DNA methylation above the genomic average.

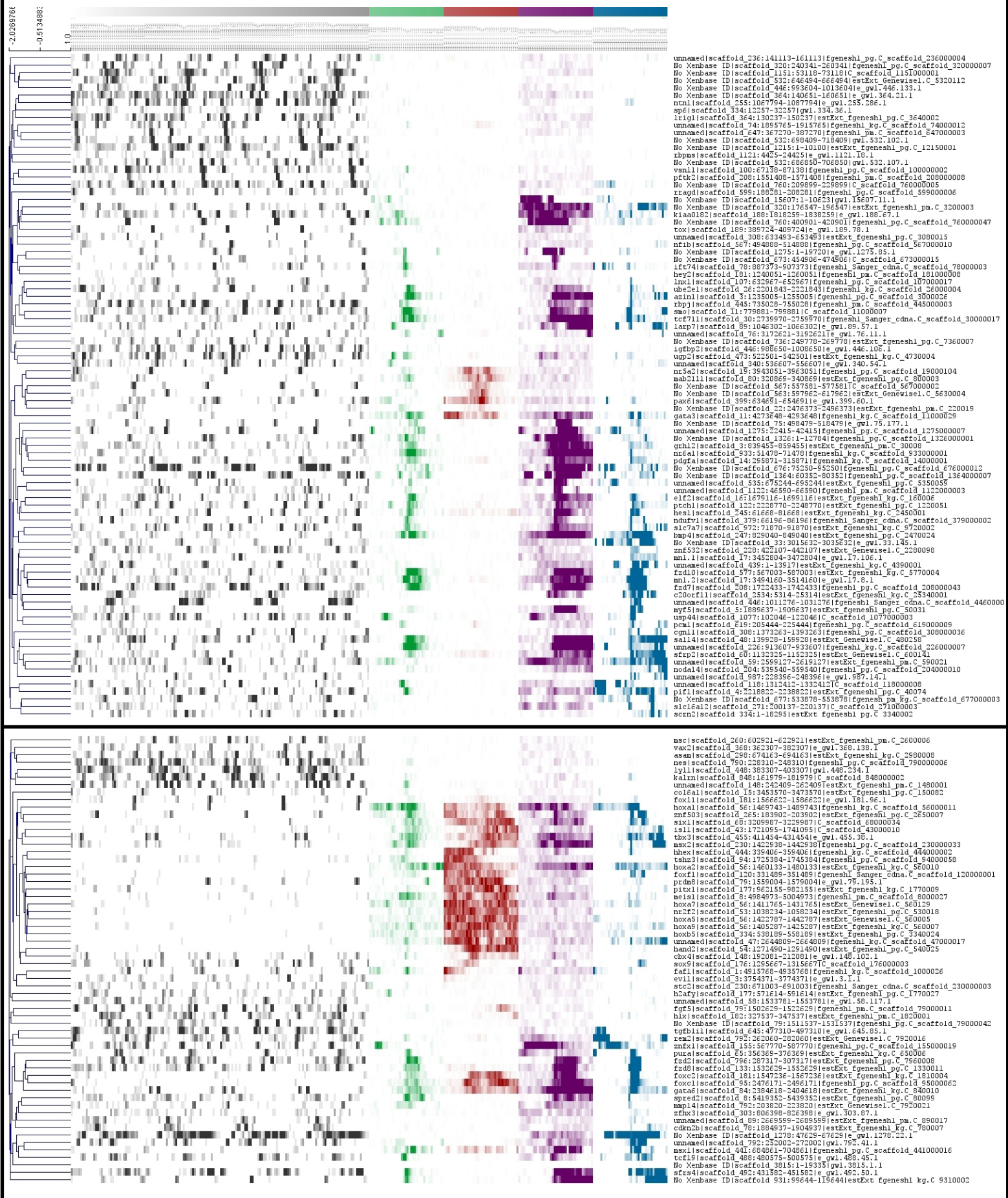


Figure S9. Companion figure of figure 5B. Gene names (if available) and genomic positions of the loci are indicated on the right side of the figure. Hierarchical clustering performed on Xenopus orthologs of H1_exp and Fib_exp genes shows an inverse relationship between DNA methylation and H3K27me3. Also, high levels of DNA methylation are present on promoters of robustly expressed H1_exp orthologs. The upper panel corresponds to H1_exp genes and the lower one to Fib_exp genes (cf. Figure 5B).

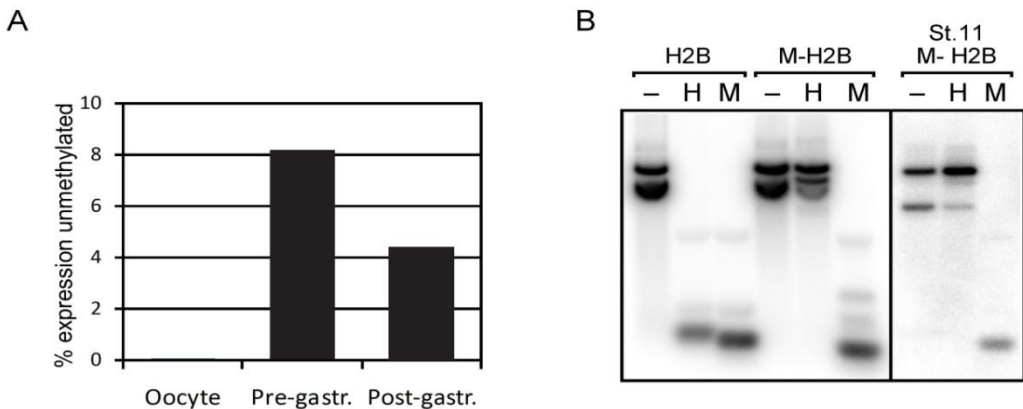


Figure S10. Activity of fully methylated H2B promoter in oocytes and embryos (transient assay). **(A)** An SssI methylated H2B promoter driving luciferase expression is very effectively (> 10,000-fold) repressed in oocytes as determined by luciferase activity. However, in embryos DNA methylation-mediated repression of transcription was severely deficient. Though in a series of independent experiments the methylated promoter template produced approximately 10-fold less luciferase than an unmethylated H2B promoter, in all cases methylated promoters produced more reporter in the first 30 to 60 minutes after the onset of embryonic transcription than during 24 hours in the oocyte. **(B)** Analysis of DNA methylation by digestion with HpaII (H, methylation-sensitive) and MspI (M, methylation-insensitive) followed by Southern blotting. Left panel: Unmethylated and SssI-methylated H2B-Luc plasmid. Right panel: The SssI-methylated template was still fully methylated when isolated from gastrula stage (stage 11) embryos, showing that the activity of the template is not due to demethylation *in vivo*.

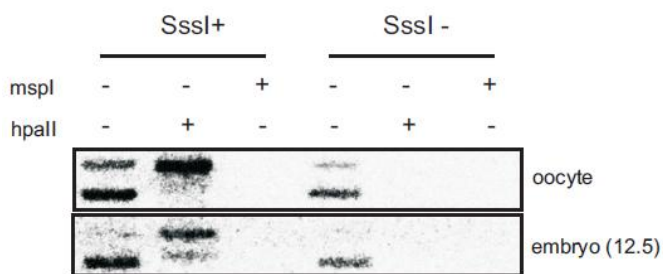
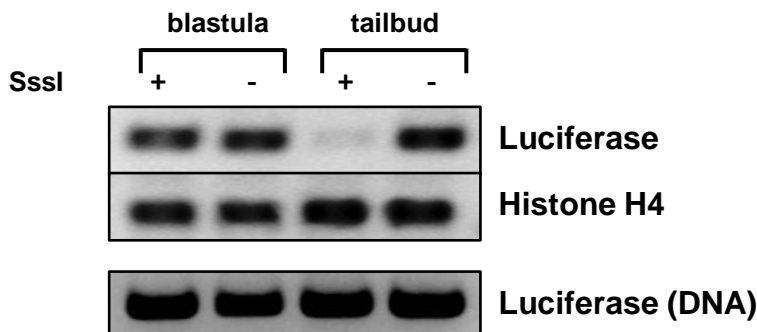
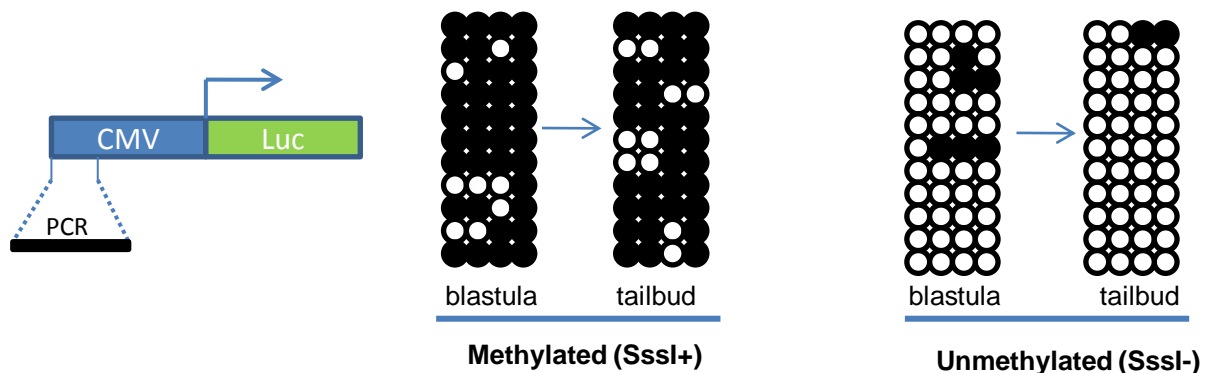


Figure S11 Southern blotting of Hsp70 plasmid DNA recovered from gastrula embryos. Both the methylated (SssI+) and the unmethylated (SssI -) plasmid are efficiently recovered from gastrula embryos with the same methylation status they had prior to injection. While both plasmids get digested by MspI, only the unmethylated plasmid will be sensitive to HpaII digestion therefore proving that methylation of the SssI + plasmid was not lost during early development. DNA was recovered from 5 embryos (2,5 ng)

A



B

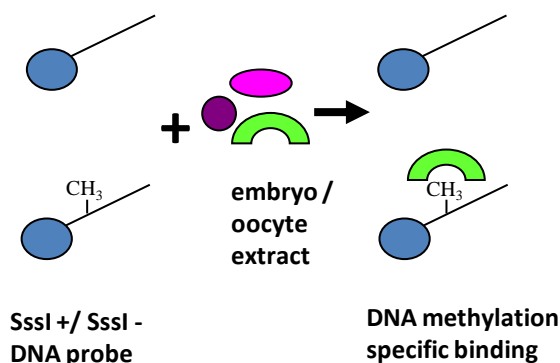


C

luc_BS2_F	AATTTAATATGGTGGATTGGATT
luc_BS2_R	AATAAACCCCTCCCCAATTAAC

Figure S12. Activity and DNA methylation of transgenes stably integrated using the Scel meganuclease protocol. **(A)** Presence of Luciferase RNA at two developmental stages (blastula and tailbud). Methylated (Sssi+) or unmethylated (Sssi-) CMV-Luc constructs were coinjected at one-cell stage embryos together with a reporter driving GFP expression. Transgenic embryos expressing GFP were selected and their DNA and RNA isolated at either blastula or tailbud stages. RNA was reverse transcribed and semi-quantitative RT-PCR (upper panel) was performed using primers for the Luc transgene and the endogenous histone H4 (loading control) gene. The lower panel shows PCR amplification of the integrated transgene from genomic DNA demonstrating that the transgenesis worked with equal efficiency in all samples. Similar to the result obtained using (Fig. 6B) a different transgenesis method (REMI) both methylated and unmethylated transgenes are expressed at the blastula stage. The methylated transgene, however, gets repressed at the tailbud stage confirming our previous observations that the uncoupling of DNA methylation and transcriptional repression is a temporal phenomenon observed only during early development. **(B)** Bisulfite sequencing of the CMV promoter controlling the Luc transgene at two developmental stages. Genomic DNA from at least 10 embryos was bisulfite treated using the EpiTect kit (QIAGEN) and subjected to PCR amplification. The PCR amplicons were cloned into the TOPO vector and sequenced. DNA methylation profiles of four CpGs located in the CMV promoter demonstrate that the methylation of the CMV promoter is preserved during blastula and tailbud stages. **(C)** primer sequences used for bisulfite sequencing of the CMV promoter.

A



B

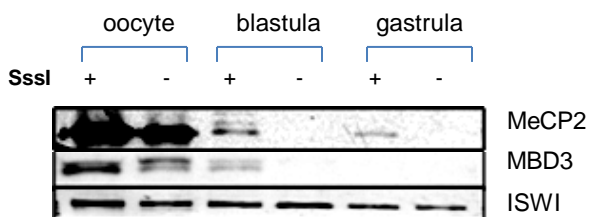
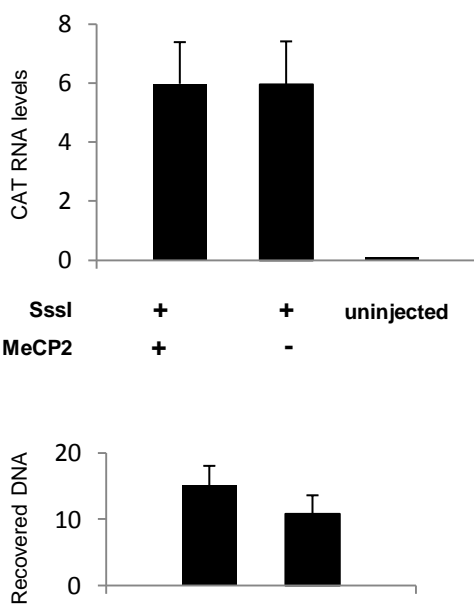


Figure S13. (A) Sssi/ methylated or unmethylated, concatamerized DNA probe was immobilized on magnetic beads and incubated with oocyte or embryo extracts. The bound fraction was eluted and analyzed by western blotting for the presence of MeCP2 and MBD3. (B) Although strongly bound in the oocyte, both of the proteins are present on methylated DNA at very low levels in the gastrulating embryo. MeCP2 is highly enriched on methylated and unmethylated DNA in the oocyte, with low but DNA methylation-selective binding at blastula and gastrula stages. MBD3 binds methylated DNA in a similar fashion, with the highest enrichment in the oocyte, a decrease in the late blastula towards a complete absence in the late gastrula. The nucleosomal ATPase ISWI was used as a positive control since its binding properties do not depend on the methylation status of the probe

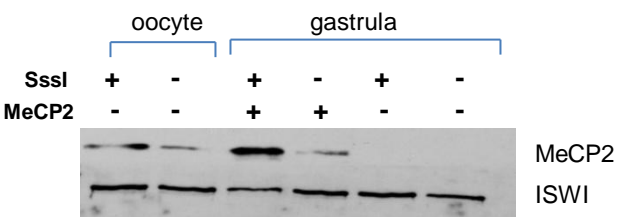
A



B



C



Figures S14. (A) Synthetic MeCP2 RNA was expressed *in vitro* and injected into *Xenopus* embryos together with a previously Sssi/ treated (methylated) hsp70 template. CAT expression was almost identical between the MeCP2 injected and uninjected sample. Plasmid DNA isolation from injected embryos shows similar recovery between the two samples. (B) MeCP2 protein expression in the injected sample was confirmed by western blotting. (C) Overexpressed MeCP2 from gastrula embryos can bind immobilized methylated DNA probes and the levels of MeCP2 present on methylated DNA correspond well to the levels observed in the oocyte.

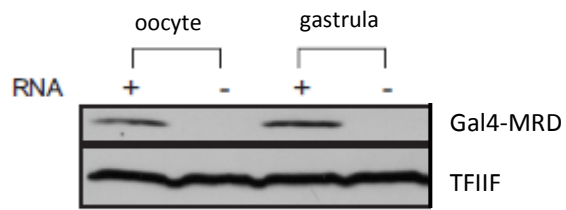


Figure S15. Western blotting of protein extracts from either Gal4-TRD RNA injected or uninjected oocytes and gastrula embryos. Gal4-TRD RNA is translated with equal efficiency in oocytes and embryos. TFIIF was used as loading control.